Electronic Supplementary Material (ESI) for Catalysis Science & Technology.


# Double Local Electromagnetic Field Collaboratively Enhanced Triplet-triplet Annihilation Upconversion for Efficient photocatalysis

Jiaojiao Fang [a,b*], Chengyang Zhu [a], Yaru Ni [b], Chunhua Lu [b*] and Zhongzi Xu [b]

[a]*Key Laboratory of Functional Molecular Solids Ministry of Education, College of Chemistry and Materials Science, Anhui Normal University, Wuhu 241002, China.*

[b]*College of Materials Science and Engineering, State Key Laboratory of Materials-Orient Chemical Engineering, Jiangsu Collaborative Innovation Center for Advanced Inorganic Function Composites, Jiangsu National Synergetic Innovation Center for Advanced Materials (SICAM), Nanjing Tech University, Nanjing 210009, P.R. China.*

***Corresponding Author***

** Dr. Jiaojiao Fang (E-mail: JJFang@ahnu.edu.cn).*

** Prof. Chunhua Lu (E-mail: chhlu@njtech.edu.cn).*

1. Preparation of $SiO_2$ nanoparticles

$SiO_2$ nanoparticles were synthesized by a modified Stober method [1]. Firstly, A solution containing DI water, ethanol and $NH_4OH$ as well as B solution composed of tetraethyl orthosilicate and ethanol were prepared and stirred for 30 min, respectively. Subsequently, solution B was added into solution A quickly under a stirring speed of 800 rpm. Then the stirring speed was changed to 500 rpm. After the reaction for 2 h at room temperature, $SiO_2$ nanoparticles were collected by centrifugation and washed with ethanol for three times.

2. Photocatalytic $CO_2$ reduction test

The photocatalytic films were placed in a circulation system with $H_2O$ and triethanolamine solution (TEOA, 10 vt%), respectively. After vacuuming the system, $CO_2$ was introduced to measure the photocatalytic $CO_2$ reduction under xenon lamp radiation (300 W). The produced gas (1 mL) was directly collected at the irradiation time of 10 h and then analyzed by a gas chromatography system.

3. Simulations

The finite-difference-time-domain method (FDTD, DongJun Technology) was used to simulate the electric field distribution in upconversion films. Different theoretical models of 3D photonic crystals can be obtained by setting the number of the array and the diameters of the spheres. The calculation conditions were set as follows: Gaussian wave was chosen as the excitation source with the propagation direction from top to bottom. The mesh size was set as 30 per wavelength. The boundary conditions of X and Z directions were Bloch conditions while the Y direction was open boundary condition. The recorded frequency range was from 300 to 1000 THz with a 20 THz per step.

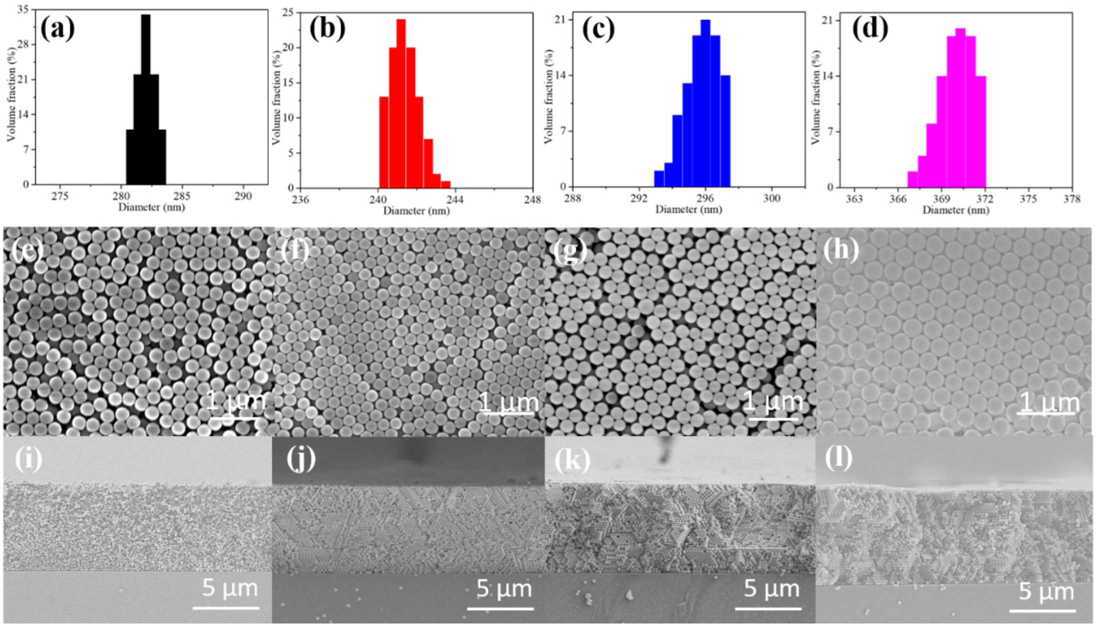


Fig. S1 Diameter distribution, surface FESEM images and cross section FESEM images of (a, e, i) $SiO_2$-625, (b, f, j) $SiO_2$-545, (c, g, k) $SiO_2$-670 and (d, h, l) $SiO_2$-800.

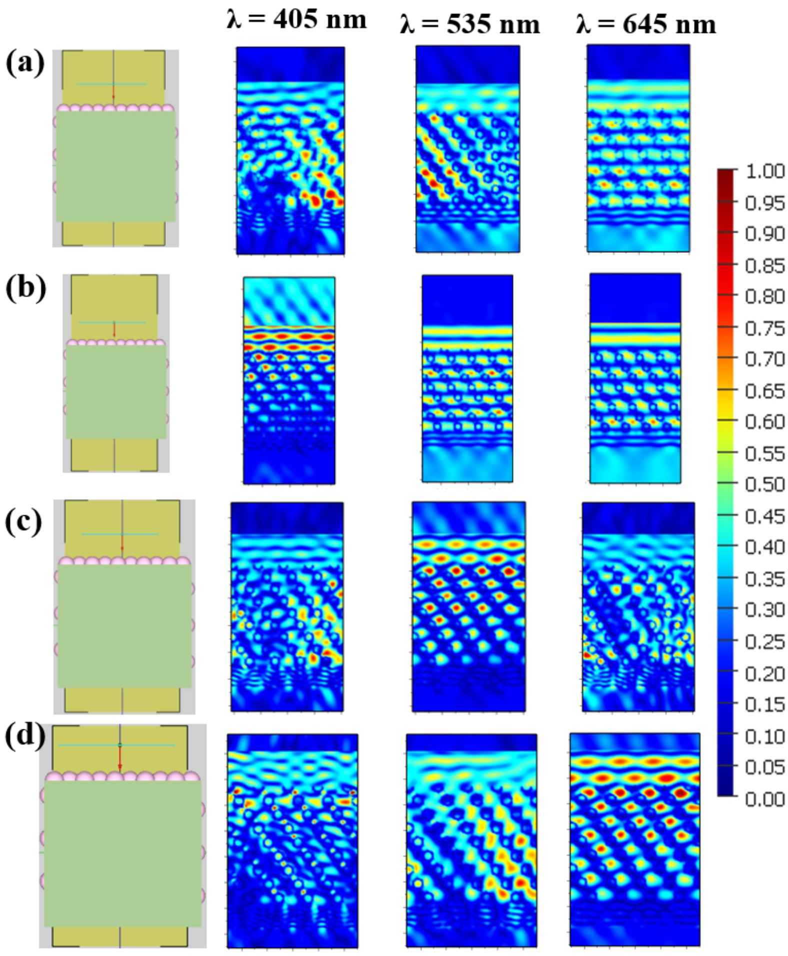


Fig. S2 The electromagnetic field distributions of samples, (a) IO625-PtDPAPV, (b) IO545-PtDPAPV, (c) IO670-PtDPAPV and (d) IO800-PtDPAPV.

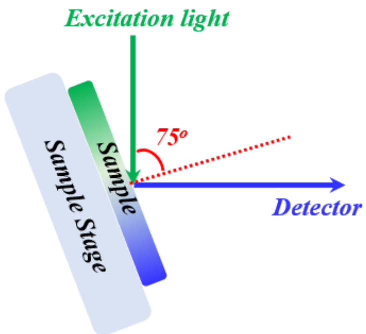


Fig. S3 The schematic diagram of the position for samples with the spectrofluorometer.

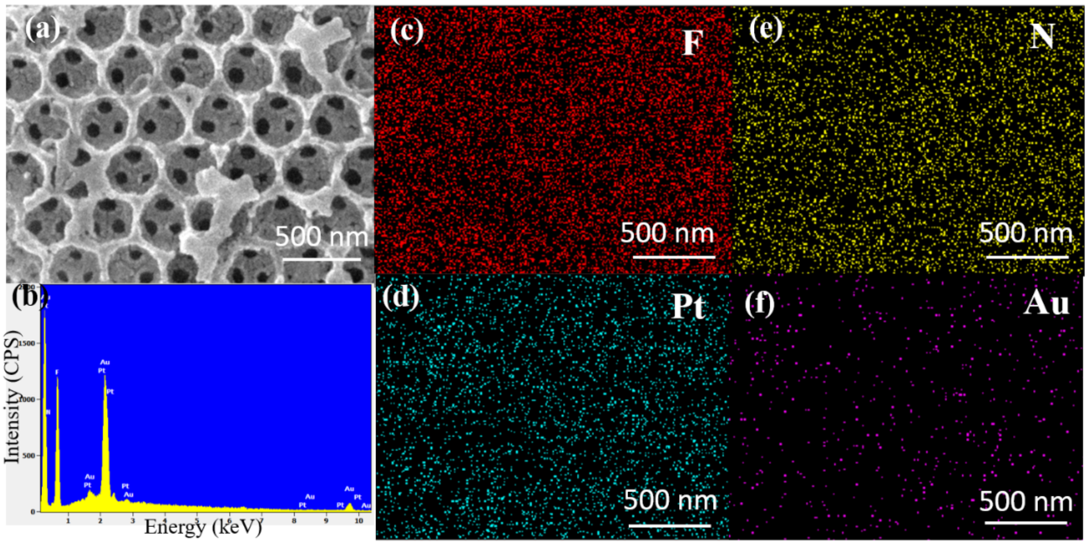


Fig. S4 (a) FESEM image and (b) The EDS spectrum of IO670-0.3 AuNPs-PtDPAPV. (c-f) elements SEM mapping.

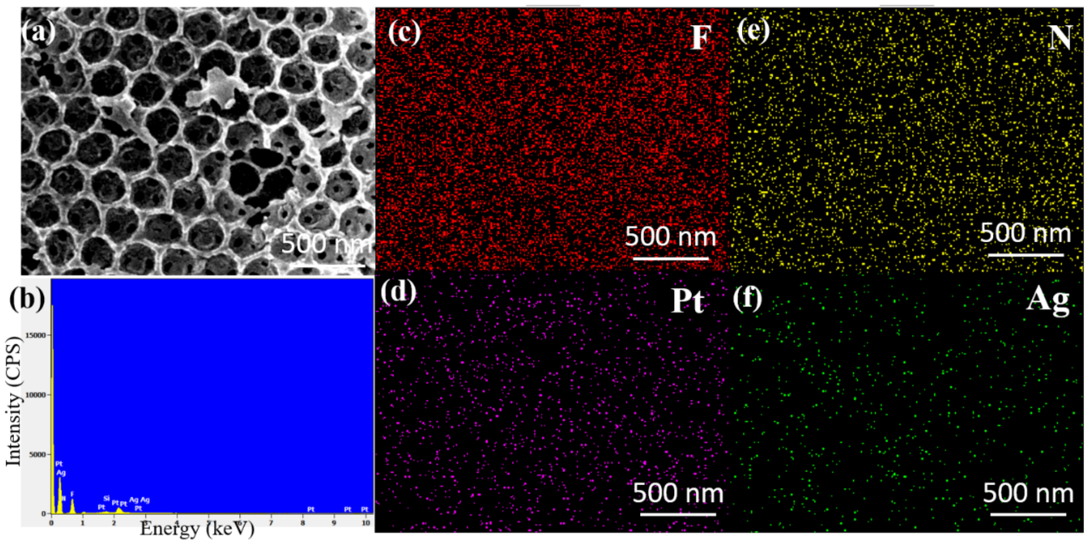


Fig. S5 (a) FESEM image and (b) The EDS spectrum of IO545-0.3 AgPl-PtDPAPV. (c-f) elements SEM mapping.

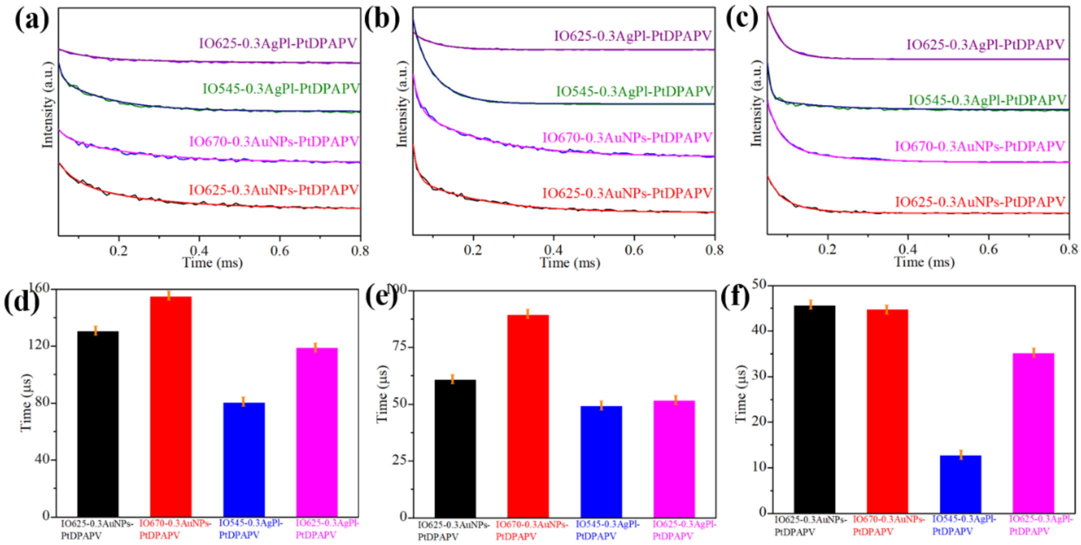


Fig. S6 (a) TTA-UC fluorescence lifetime spectra and (d) lifetime average value of samples at 405 nm ($\lambda_{ex}$=535 nm). (b) Phosphorescence lifetime spectra and (e) lifetime average value of samples at 645 nm ($\lambda_{ex}$=535 nm). (c) Emission lifetime spectra of samples and (f) lifetime average value at 405 nm ($\lambda_{ex}$=360 nm).

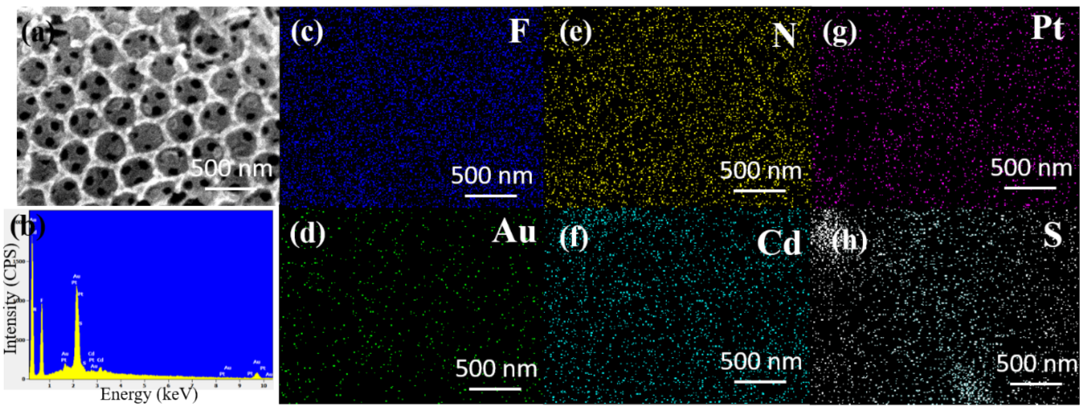


Fig. S7 (a) FESEM image and (b) The EDS spectrum of IO670-0.3 AuNPs-PtDPAPV/3CdS. (c-h) elements SEM mapping.

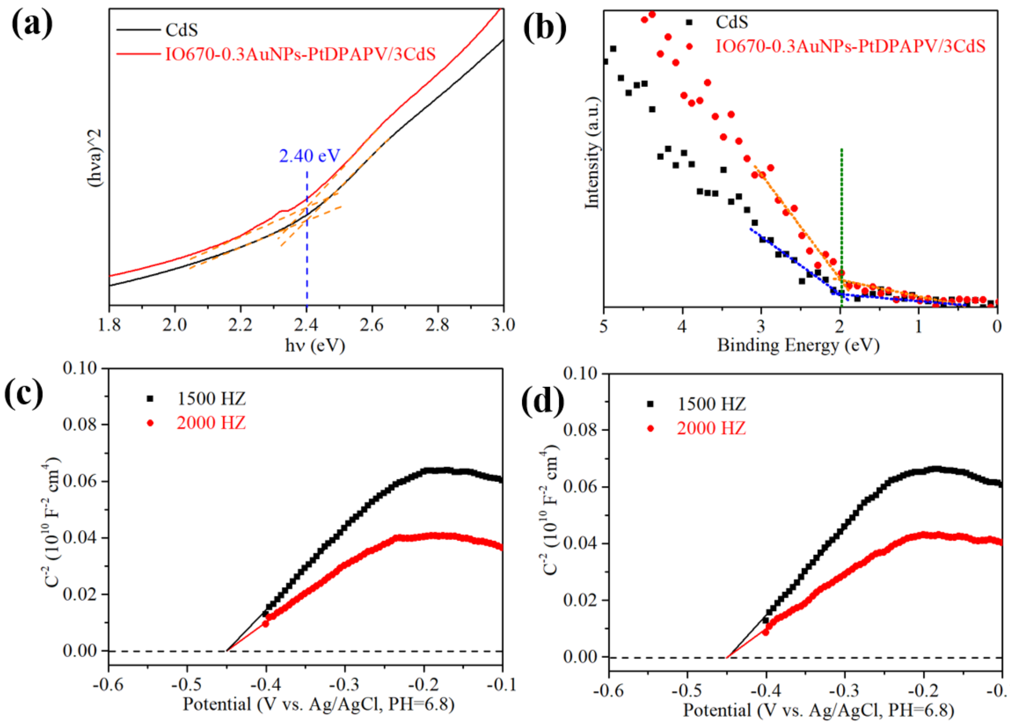


Fig. S8 (a) Tauc plots, (b) VB spectra of samples and Mott-Schottky plots of (c) CdS and (d) IO670-0.3AuNPs-PtDPAPV/3CdS.

The Tauc plots, VB spectra of samples and Mott-Schottky plots were used to measure the band structures of photocatalysts (Fig. S8). The samples have the same band gap widths of 2.40 eV (Fig. S8a). Moreover, the onsets of CdS and IO670-0.3AuNPs-PtDPAPV/3CdS are both 1.98 eV (Fig. S8b). Additionally, the flatband potential of CdS is the same as that of IO670-0.3AuNPs-PtDPAPV/3CdS (Figs. S8c-d). These results suggest that 0.3AuNPs-PtDPAPV has a negligible effect on the band structures of CdS.

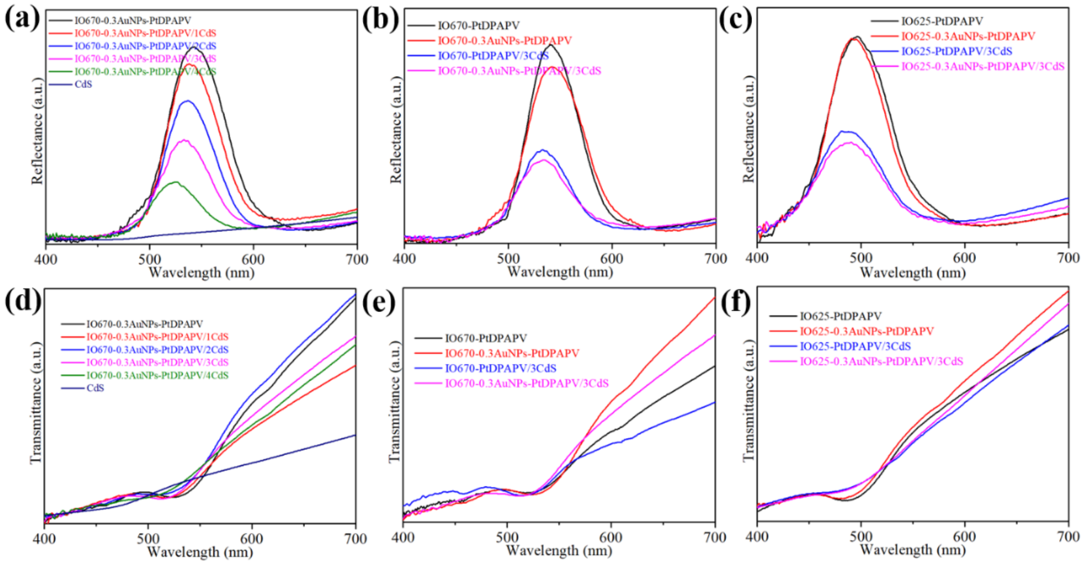

Fig. S9 (a-c) Reflectance and (d-f) transmittance spectra of samples.

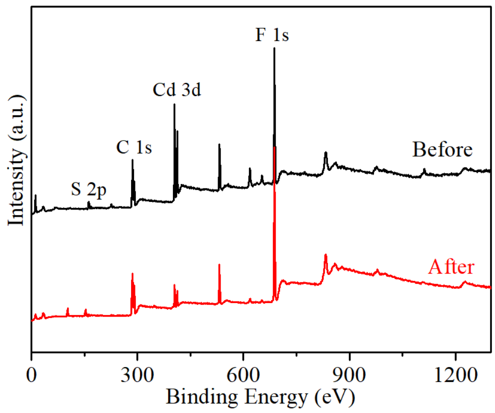


Fig. S10 The XPS spectra of IO670-0.3 AuNPs-PtDPAPV/3CdS.

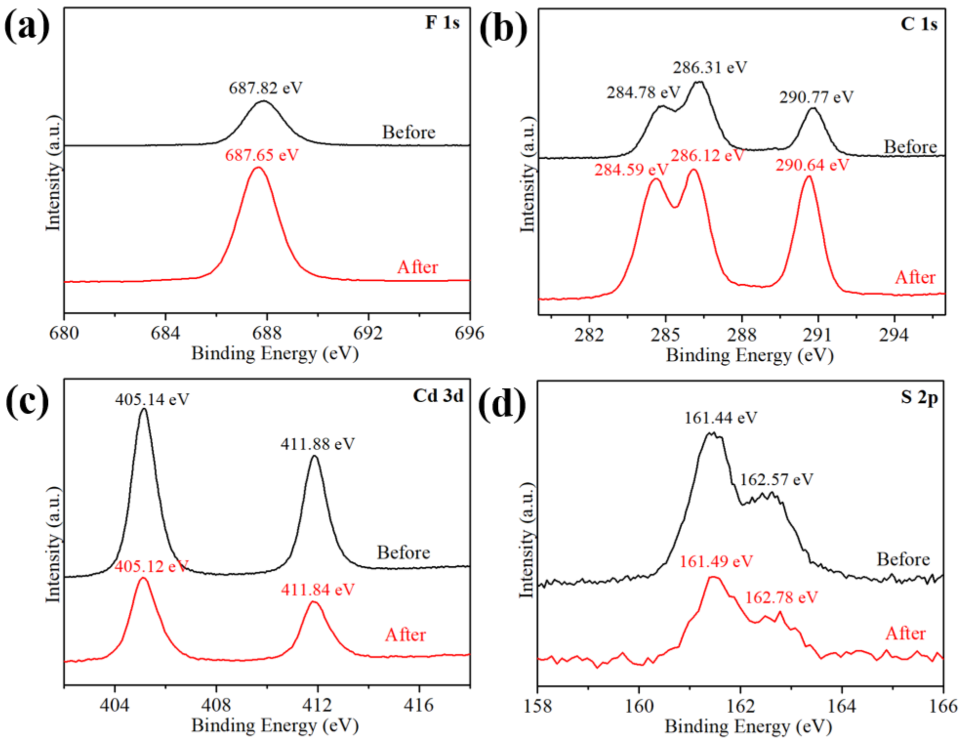


Fig. S11 (a) F 1s, (b) C 1s, (c) Cd 3d and (d) S 2p XPS spectra of IO670-0.3 AuNPs-PtDPAPV/3CdS.

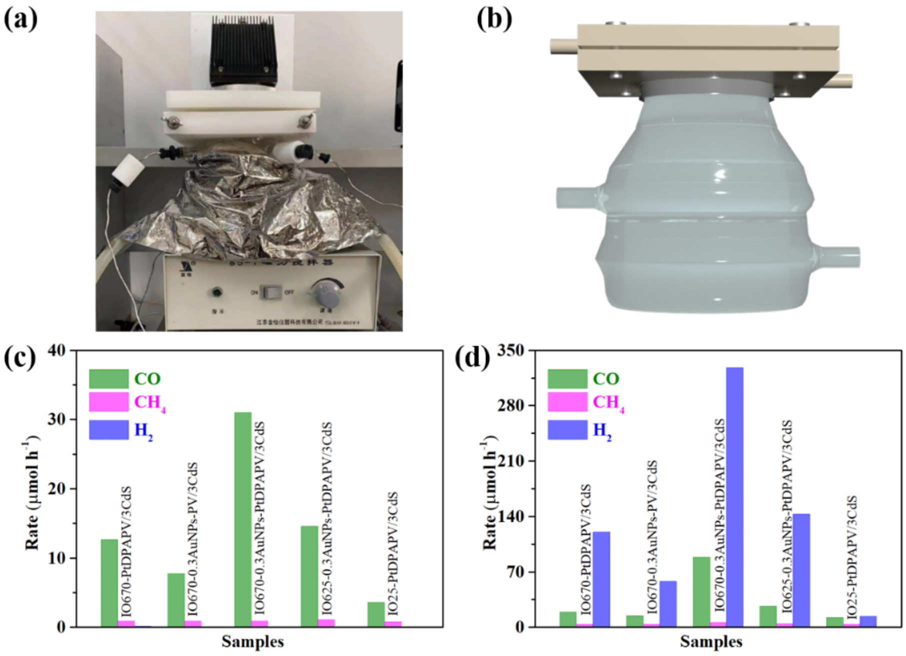


Fig. S12 The picture (a) and schematic (b) of the device for photocatalytic reduction of carbon dioxide. Photocatalytic $CO_2$ reduction rates of samples (c) without TEOA and (d) with TEOA as a sacrifice agent under xenon light irradiation.

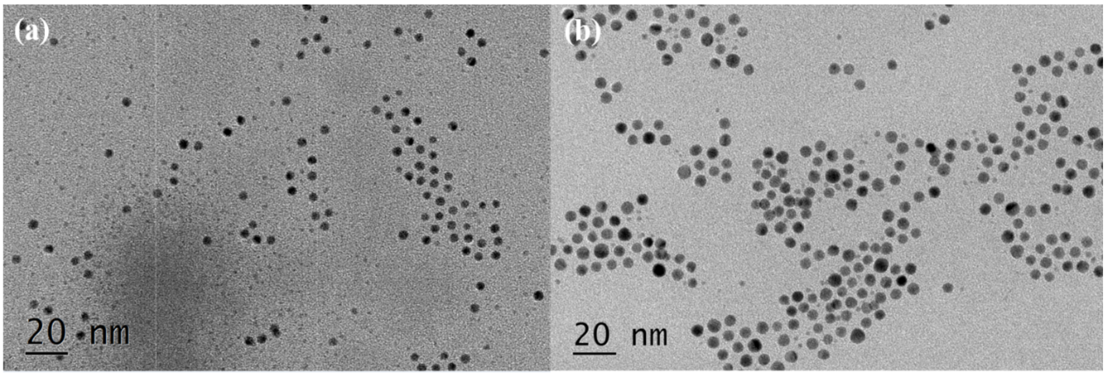


Fig. S13 TEM images of (a) AuNPs and (b) AgPl.

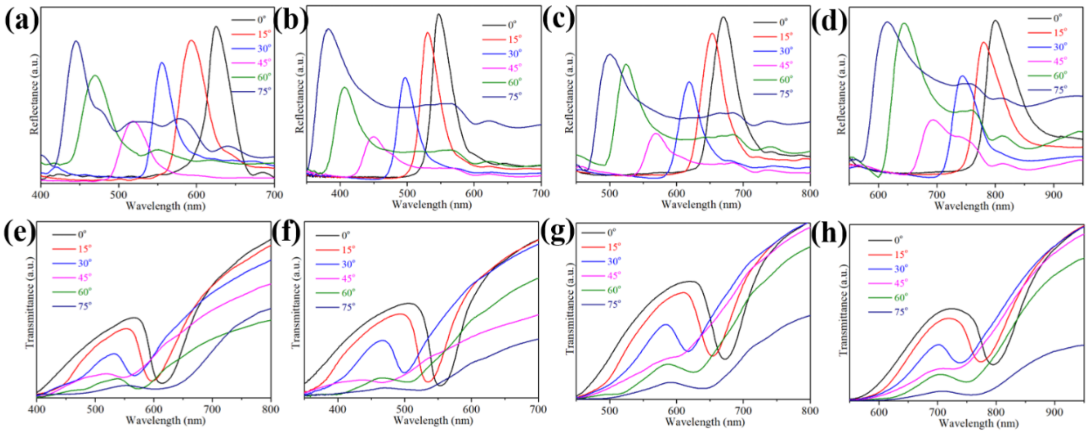


Fig. S14 Reflectance spectra of (a) $SiO_2$-625, (b) $SiO_2$-545, (c) $SiO_2$-670 and (d) $SiO_2$-800.

Transmittance spectra of (e) $SiO_2$-625, (f) $SiO_2$-545, (g) $SiO_2$-670 and (h) $SiO_2$-800.

# References

1 C. Zhu, J. Fang, Y. Ni, L. Fang, C. Lu, Z. Xu and Z. Kang, *J Mater Sci: Mater Electron*, 2018, **29**, 1680-1689.